The Company of
Biologists

RESEARCH REPORT

osr1 couples intermediate mesoderm cell fate with temporal dynamics of vessel progenitor cell differentiation

Elliot A. Perens[1,2,*], Jessyka T. Diaz[1,2], Agathe Quesnel[1], Amjad Askary[3], J. Gage Crump[3] and Deborah Yelon[1,*]

ABSTRACT

Transcriptional regulatory networks refine gene expression boundaries to define the dimensions of organ progenitor territories. Kidney progenitors originate within the intermediate mesoderm (IM), but the pathways that establish the boundary between the IM and neighboring vessel progenitors are poorly understood. Here, we delineate roles for the zinc-finger transcription factor Osr1 in kidney and vessel progenitor development. Zebrafish *osr1* mutants display decreased IM formation and premature emergence of lateral vessel progenitors (LVPs). These phenotypes contrast with the increased IM and absent LVPs observed with loss of the bHLH transcription factor Hand2, and loss of *hand2* partially suppresses *osr1* mutant phenotypes. *hand2* and *osr1* are expressed together in the posterior mesoderm, but *osr1* expression decreases dramatically prior to LVP emergence. Overexpressing *osr1* during this timeframe inhibits LVP development while enhancing IM formation, and can rescue the *osr1* mutant phenotype. Together, our data demonstrate that *osr1* modulates the extent of IM formation and the temporal dynamics of LVP development, suggesting that a balance between levels of *osr1* and *hand2* expression is essential to demarcate the kidney and vessel progenitor territories.

KEY WORDS: Zebrafish, Intermediate mesoderm, Kidney, Vessel progenitors, *hand2*

INTRODUCTION

Proper embryonic patterning depends on the establishment of progenitor territories with well-defined gene expression patterns (Briscoe and Small, 2015). For example, the medial-lateral axis of the vertebrate posterior mesoderm is divided into precise stripes of progenitor territories that give rise to various organs and cell types, including the kidneys, blood vessels and blood cells (Prummel et al., 2020). Kidney progenitors originate within a pair of bilateral territories called the intermediate mesoderm (IM) (Davidson et al., 2019; Dressler, 2009; Gerlach and Wingert, 2013). Across species, the dimensions of the IM are defined by the expression of conserved transcription factors, such as Lhx1/Lim1 and Pax2, that are required for its development (Carroll et al., 1999; Cirio et al., 2011; Torres et al., 1995; Tsang et al., 2000), but the mechanisms that establish boundaries between the IM and its neighboring territories remain poorly understood.

The zinc-finger transcription factor Osr1 is an intriguing candidate for playing a central role in IM boundary formation. Gene expression analyses and temporal fate mapping in amniotes demonstrated that *Osr1* is expressed initially in the IM and the laterally adjacent mesoderm, which contains vessel progenitors, before its expression becomes restricted to kidney progenitors (James et al., 2006; Mugford et al., 2008). In zebrafish, *osr1* is expressed in the posterior mesoderm, initially adjacent to the IM; later, a stripe of lateral vessel progenitors (LVPs) arises between the IM and the *osr1*-expressing territory (Mudumana et al., 2008; Perens et al., 2016). Mouse *Osr1* knockout embryos have decreased *Lhx1* and *Pax2* expression during early stages of kidney development, thought to be due to increased apoptosis (Wang et al., 2005). In zebrafish, *osr1* knockdown studies yielded varying conclusions: one study of *osr1* morphants determined that *osr1* is only required for maintenance of the pronephron lineage (Mudumana et al., 2008), while another indicated that *osr1* was required for IM formation (Tena et al., 2007). Additionally, *osr1* knockdown resulted in an expanded venous vasculature (Mudumana et al., 2008). As cell tracking experiments have shown that LVPs contribute to the cardinal vein (Kohli et al., 2013), it is interesting to consider whether *osr1* may influence LVP development. In total, however, the functions of *osr1* in the initial development of the IM and vessel progenitors remain unclear.

Considering the discrepancies often seen between morphants and mutants (Schulte-Merker and Stainier, 2014), we chose to augment previous *osr1* morphant studies (Mudumana et al., 2008; Tena et al., 2007; Tomar et al., 2014) by analyzing a TALEN-generated *osr1* mutation (Askary et al., 2017). The *osr1* mutant phenotype demonstrated important roles of *osr1* in promoting IM and pronephron differentiation and inhibiting premature LVP formation. Previously, we have found that *osr1* and *hand2*, which encodes a bHLH transcription factor, are co-expressed in the most lateral territory of the posterior mesoderm and that *hand2* promotes LVP development while inhibiting the lateral extent of IM formation (Perens et al., 2016). Each of these phenotypes was partially suppressed by mutation of *osr1*. Intriguingly, wild-type embryos displayed a striking reduction of *osr1* expression immediately before LVP formation, and overexpression of *osr1* inhibited LVP emergence while elevating IM formation. Together, our studies suggest a new model in which *osr1* expression dynamics balance IM differentiation with the temporal emergence of neighboring vessel progenitors.

RESULTS AND DISCUSSION
Mutation of *osr1* has graded effects along the proximal-distal axis of the pronephron

To enhance our understanding of *osr1* function in the posterior mesoderm, we analyzed a TALEN-generated *osr1* mutation

[1]Division of Biological Sciences, University of California, San Diego, La Jolla, CA 92037, USA. [2]Division of Pediatric Nephrology, Department of Pediatrics, University of California, San Diego, La Jolla, CA 92037, USA. [3]Eli and Edythe Broad Center for Regenerative Medicine and Stem Cell Research, University of Southern California, Los Angeles, CA 90033, USA.

*Authors for correspondence (eperens@health.ucsd.edu; dyelon@ucsd.edu)

E.A.P., 0000-0003-3377-7708; D.Y., 0000-0003-3523-4053

DEVELOPMENT

(Askary et al., 2017). *osr1^{el593}* is a 7 bp deletion leading to a frameshift; the predicted mutant Osr1 protein would contain its first 80 amino acids, followed by 45 missense amino acids, and would lack its zinc fingers (Fig. 1A). Thus, *osr1^{el593}* is likely a strong loss-of-function allele.

Homozygous *osr1* mutant embryos exhibited progressive pericardial and body edema (Fig. 1B,C) comparable with other zebrafish mutants with defects in pronephron development (Kroeger et al., 2017; Lun and Brand, 1998). Consistent with this, *osr1* mutants displayed deficits in multiple pronephron segments. Most dramatically, markers of the glomerular precursors (*wt1b*, Fig. 1F) and glomerular precursors and neck region (*pax2a*, Fig. S1B) were absent. *cdh17*, which is normally expressed throughout the pronephron tubules (Fig. 1I), lacked expression at the proximal extent of the tubule, while the remaining tubule appeared thinner (Fig. 1J). Similarly, a marker of the proximal convoluted tubule segment (*slc20a1a*, Fig. 1M,N) was reduced in intensity, while a marker of the distal late segment

(*slc12a3*, Fig. 1Q,R) revealed a slightly thinner expression pattern in the mutant. Thus, although previous morphant studies found that *osr1* is required for only proximal tubule development (Mudumana et al., 2008), the *osr1* mutant phenotype revealed that *osr1* is required for development of the entire pronephron but has a higher impact on the development of the proximal territories.

The proximal deficiencies observed in *osr1* mutants were reminiscent of the pronephron phenotypes previously shown to result from overexpression of *hand2* (Perens et al., 2016). Additionally, pronephron size was increased in a *hand2* null mutant (Perens et al., 2016) (Fig. 1G,K,O,S), and knockdown of *osr1* function partially suppressed this *hand2* mutant phenotype (Perens et al., 2016). Similarly, we found that mutation of *osr1* partially suppressed the pronephron phenotypes in *hand2* mutants (Fig. 1H,L,P,T; Fig. S1D). Confirmation of this genetic interaction during pronephron development raised the possibility that *osr1*, like *hand2*, regulates IM formation.
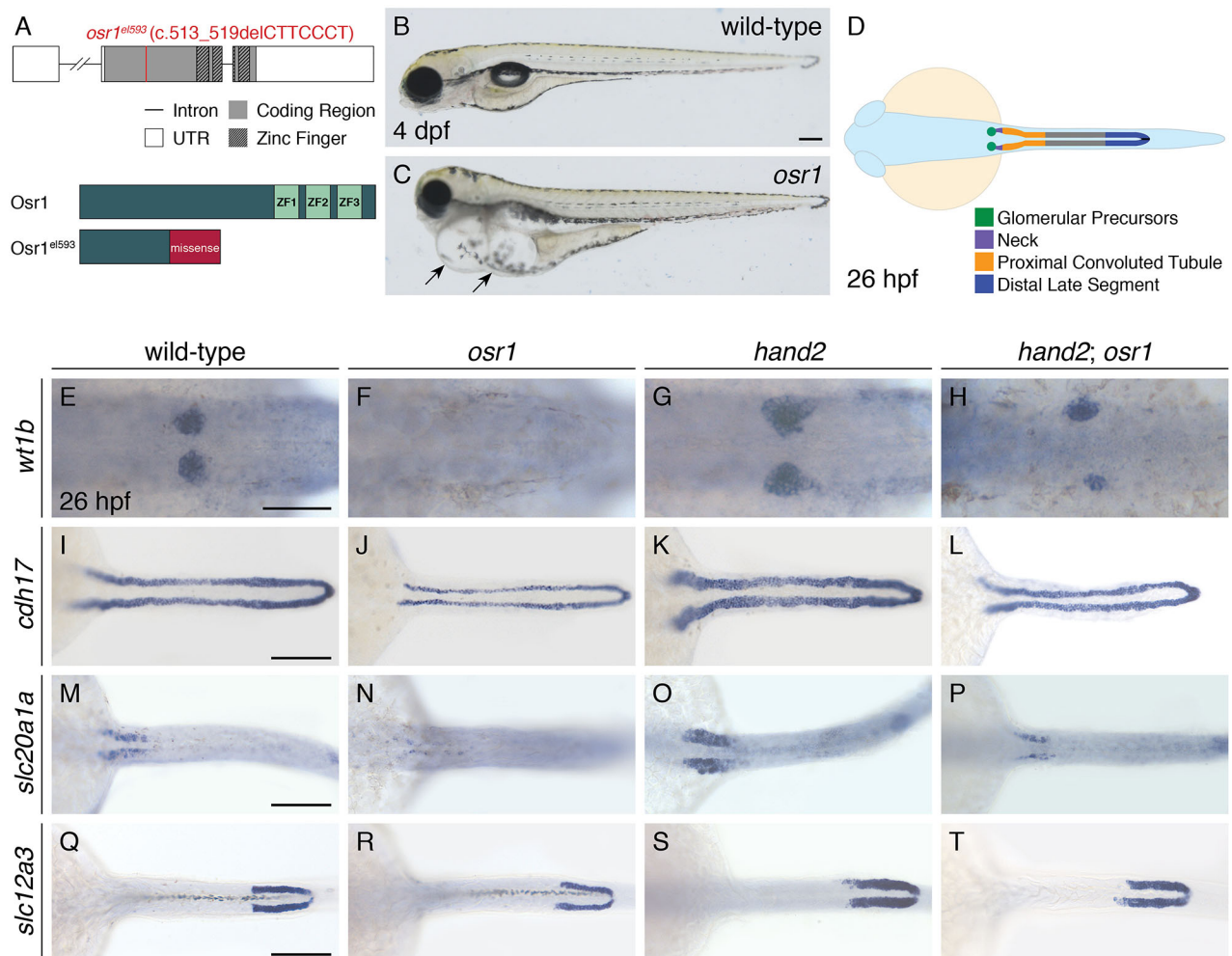
Fig. 1. Pronephron defects in *osr1* mutants are partially suppressed by *hand2* loss of function. (A) *osr1^{el593}* is a TALEN-generated 7 bp deletion allele. Schematics show gene structure with location of deletion, and predicted wild-type and Osr1^{el593} proteins (ZF, zinc finger). (B,C) Lateral views, anterior to the left, of wild-type (B) and *osr1* mutant (C) embryos at 4 days post-fertilization (dpf). *osr1* mutants display severe pericardial and body wall edema (arrows). (D-T) Dorsal views, anterior to the left, of a pronephron schematic (D), and wild-type (E,I,M,Q), *osr1* mutant (F,J,N,R), *hand2* mutant (G,K,O,S) and *hand2*; *osr1* double mutant (H,L,P,T) embryos at 26 h post-fertilization (hpf). *In situ* hybridization shows expression of *wt1b* (E-H) in glomerular precursors, *cdh17* (I-L) throughout the tubules, *slc20a1a* (M-P) in the proximal convoluted tubules, and *slc12a3* (Q-T) in the distal late segments. Compared with wild type (E,I,M,Q), expression is absent (F), thin and shortened anteriorly (J), reduced (N), and thin (R) in *osr1* mutants; expanded in *hand2* mutants (G,K,O,S); and relatively similar to wild type in *hand2*; *osr1* double mutants (H,L,P,T). Scale bars: 200 µm (B,C); 100 µm (I-T); 25 µm (E-H).

osr1 is required to generate the full complement of intermediate mesoderm

Previously, we found that *hand2* constrains the size of the pronephron by repressing IM formation (Perens et al., 2016). We therefore investigated whether *osr1* also regulates the extent of initial IM formation. We observed narrowed expression of *lhx1a* in the *osr1* mutant IM, in comparison with the wild-type IM (Fig. 2A,B), and this aspect of the *osr1* mutant phenotype could be rescued by injection of wild-type *osr1* mRNA (Fig. S2). Quantification of the number of Pax2a⁺ cells revealed that the altered IM appearance in *osr1* mutants reflected a significant decrease in the number of IM cells (Fig. 2I). Thus, although other studies reached varying conclusions regarding an early role for *osr1* in IM formation (Drummond et al., 2020 preprint; Mudumana et al., 2008; Tena et al., 2007), our *osr1* mutant phenotype indicated that

osr1 is required for the initial generation of the full complement of IM cells. Furthermore, we found that loss of *hand2* function partially suppressed the IM defects in *osr1* mutants (Fig. 2D,H,I). Thus, *osr1* and *hand2* operate in antagonistic genetic pathways to regulate IM differentiation, raising the possibility that *osr1*, like *hand2*, may execute this function at the lateral border of the IM.

osr1 inhibits the premature emergence of lateral vessel progenitors in the posterior mesoderm

We investigated whether *osr1*, like *hand2*, might play a role in the development of the neighboring lateral vessel progenitors (LVPs). The LVPs normally arise at the lateral boundary between the IM and the *hand2*/*osr1*-expressing territory of the posterior mesoderm during a short, consistent time window, subsequent to the appearance of the earlier-arising vessel progenitors located medial
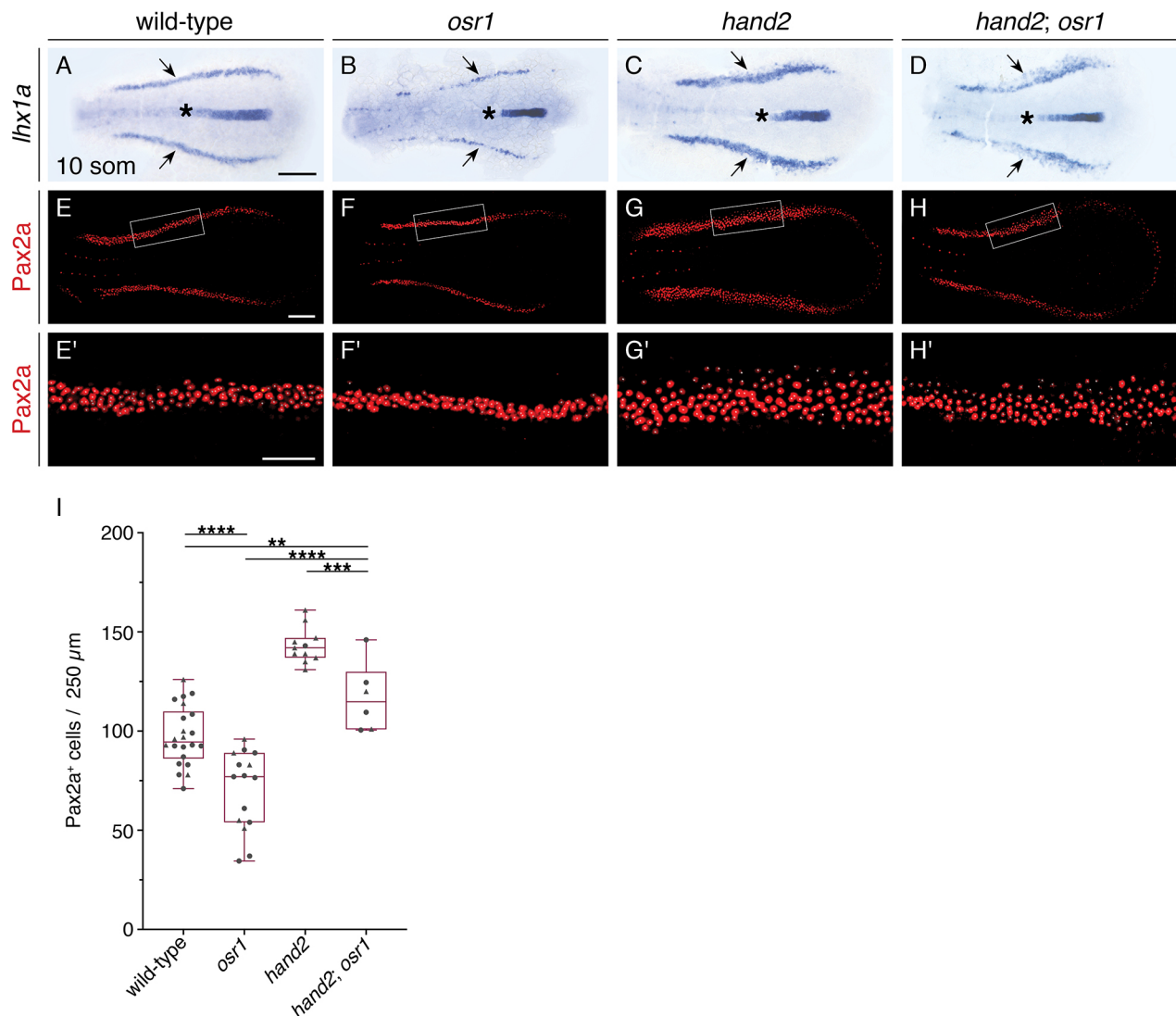
Fig. 2. *osr1* is required to promote intermediate mesoderm differentiation. (A-H) Dorsal views, anterior to the left, of the posterior mesoderm at the 10-somite stage (som). (A-D) *In situ* hybridization shows expression of *lhx1a* in the IM (arrows). Compared with wild type (A), expression is narrowed in *osr1* (B), widened in *hand2* (C) and irregular in *hand2*; *osr1* (D) embryos. Expression in the notochord (asterisk) is unaffected. Unlike the width of the IM, we did not observe a change in the proximal-distal length of the IM in mutant embryos. (E-H) Three-dimensional reconstructions of Pax2a immunofluorescence in the IM of wild-type (E), *osr1* (F), *hand2* (G) and *hand2*; *osr1* (H) embryos. (E′-H′) Magnification of boxed 250 μm long regions used for counting Pax2a⁺ cells. White dots indicate Pax2a⁺ nuclei. (I) Quantification of Pax2a⁺ cells in a 250 μm long region of the IM in the indicated genotypes. Symbols represent individual embryos (circles, average of left and right IMs; triangles, single IM; see Materials and Methods); boxes represent interquartile range; central line marks the median; whiskers indicate maximum and minimum values. *P* values were calculated using non-parametric Mann–Whitney *U*-tests: ****$P<0.0001$, ***$P=0.0011$, **$P=0.0094$. Scale bars: 100 μm (A-H); 50 μm (E′-H′).

to the IM (Kohli et al., 2013; Perens et al., 2016) (Fig. 3A,B,E). Surprisingly, we found that LVPs form prematurely in *osr1* mutants. Specifically, while *etv2*-expressing LVPs rarely appeared prior to the 10-somite stage in wild-type embryos, some *osr1* mutants exhibited *etv2*-expressing LVPs as early as the 6-somite stage, and most *osr1* mutants possessed *etv2*-expressing LVPs by the 8-somite stage (Fig. 3C-E, Fig. S3). In contrast, the timing of the appearance of medial vessel progenitors was unaffected (Fig. S4). Thus, *osr1* constrains vessel progenitor development by inhibiting the premature differentiation of LVPs at the lateral border of the IM.

Because *osr1* and *hand2* interact antagonistically during IM development, we examined whether the same genetic interaction occurs during vessel progenitor development. Notably, while *hand2* mutants rarely form LVPs (Fig. 3H; 74% have no LVPs and 26% have one to three LVPs, *n*=31) (Perens et al., 2016), more *etv2*-expressing LVPs do form in *hand2*; *osr1* double mutants (Fig. 3I;

22% have no LVPs, 56% have one to three LVPs and 22% have four to 10 LVPs, *n*=9). However, although *hand2* mutants lack expression of *flt4* and *mrc1a* within the cardinal vein (Perens et al., 2016), expression of these genes is not affected in *osr1* mutants (Fig. S5E,H). Altogether, our data suggest that, as in the IM, *osr1* and *hand2* act in antagonistic genetic pathways to regulate LVP formation.

In addition to the IM and LVP phenotypes, we found that *gata1*-expressing blood progenitors were reduced throughout the posterior mesoderm in *osr1* mutants (Fig. S6B). Unlike the IM and LVPs, however, blood progenitors did not seem altered in *hand2* mutants (Fig. S6C), and the *osr1* mutant phenotype did not appear to be suppressed by loss of *hand2* (Fig. S6D). Thus, in addition to the antagonistic pathways through which *osr1* and *hand2* regulate IM and LVP formation, *osr1* may function in additional genetic pathways that influence posterior mesoderm patterning.
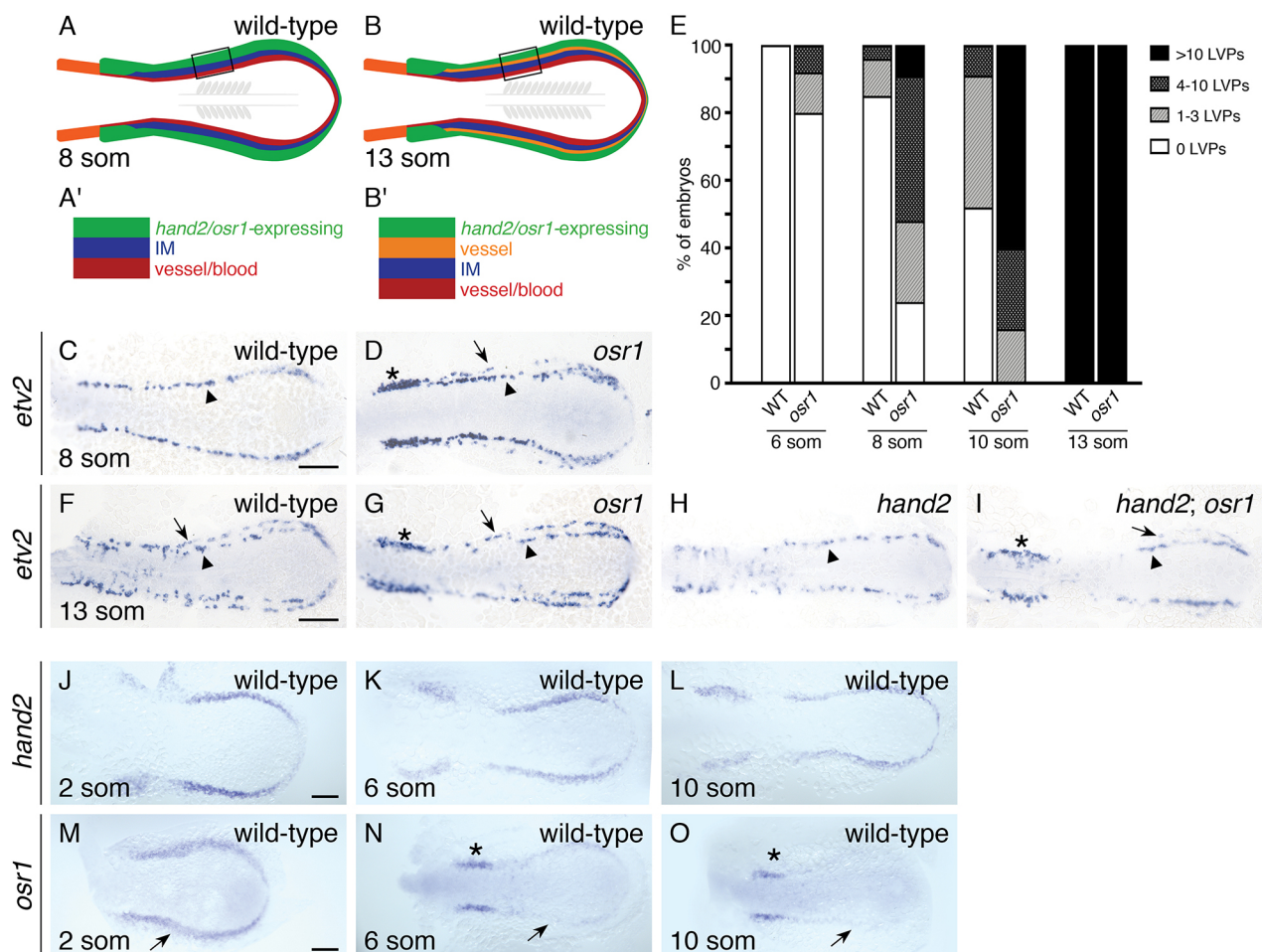
Fig. 3. *osr1* inhibits the premature emergence of lateral vessel progenitors. (A,B) Schematics depict posterior mesoderm territories, dorsal views, anterior to the left. (A′,B′) Expansion of corresponding boxed regions. (C,D,F-I) *In situ* hybridization shows *etv2* expression in wild-type (C,F), *osr1* (D,G), *hand2* (H) and *hand2*; *osr1* (I) embryos; dorsal views, anterior to the left, at the 8- (C,D) and 13- (F-I) somite stages (som). (C,D) At 8 som, *etv2* is expressed in a relatively medial territory (arrowheads) on each side of the wild-type mesoderm (C). In *osr1* mutants, *etv2* is also expressed in some relatively lateral cells (D, arrow), and its expression is increased in a distinct proximal region (asterisk). (E) Quantification of LVPs in wild-type and *osr1* mutant embryos at 6, 8, 10 and 13 som; sample sizes provided in Fig. S3E. Embryos were categorized based on the number of cells observed on whichever side of the mesoderm exhibited more LVPs. (F-I) At 13 som, *etv2* is expressed in both relatively medial (arrowheads) and lateral (arrows) territories on each side of wild-type (F), *osr1* (G) and *hand2*; *osr1* (I) embryos. In *hand2* mutants (H), *etv2* is expressed only in the medial territory. In *osr1* (G) and *hand2*; *osr1* (I) embryos, *etv2* expression is increased proximally (asterisks). (J-O) Dorsal views, anterior to the left, of *in situ* hybridization in wild-type embryos at 2 som (J,M), 6 som (K,N) and 10 som (L,O). Between 2 and 10 som, *hand2* (J-L) remains expressed in a relatively broad domain of the wild-type posterior mesoderm. In contrast, *osr1* expression is initially broad (M, arrow) but then becomes reduced in width and intensity (N,O; arrows), except proximally, where expression remains strong (asterisks), possibly representing expression in glomerular precursors (Tomar et al., 2014). Scale bars: 100 μm.

osr1 expression levels mediate intermediate mesoderm and lateral vessel progenitor cell fate decisions

Considering the dynamic nature of *Osr1* expression in amniotes (James et al., 2006; Mugford et al., 2008), we surmised that *osr1* expression in the zebrafish posterior mesoderm might also be dynamic. Indeed, unlike *hand2*, which has consistent expression in the posterior mesoderm from tailbud stage to the 10-somite stage (Fig. 3J-L), *osr1* expression decreases dramatically during this same time period and before the emergence of the LVPs (Fig. 3M-O). Thus, decreased *osr1* expression may be required for LVP emergence.

To test whether sustained *osr1* expression would alter LVP development, we used the transgene *Tg(hsp70:osr1-t2A-BFP)* to overexpress *osr1*. Strikingly, induction of *osr1* overexpression at tailbud stage could inhibit LVP formation (Fig. 4A-D, Fig. S7). Additionally, *osr1* overexpression increased the formation of medial and proximal vessel progenitors (Fig. 4B,D, Figs S5C and S7), and caused increased and ectopic expression of vascular genes (Fig. S5F,I), suggesting that *osr1* has distinct influences on different subsets of vessel progenitors. Interestingly, *osr1* overexpression resulted in a range of severity for each of these vascular phenotypes, consistent with a dependence of vessel progenitor formation on precise *osr1* expression levels (Fig. S7).

We next examined whether there was a concomitant change in the IM when LVP formation was suppressed by *osr1* overexpression. Quantification of Pax2a$^+$ cells showed a moderate, but significant, increase in the IM when *osr1* is overexpressed (Fig. 4E-G). What might be the origin of these additional IM cells? In *hand2* mutants that exhibit IM expansion and loss of LVPs, an increased number of Pax2a$^+$ cells emerge within the *hand2*-expressing territory (Fig. S8C) (Perens et al., 2016). In contrast, in *osr1*-overexpressing embryos, Pax2a expression remained excluded from the *hand2*-expressing territory (Fig. S8B). Consistent with this difference, the increase in IM generated by *osr1* overexpression was less than that generated by *hand2* loss of function (Figs 2I and 4G) (Perens et al., 2016). Together, our findings suggest that elevated *osr1* expression drives cells at the lateral IM border toward an IM fate, rather than a LVP fate. Like *hand2* loss of function, *osr1* overexpression can suppress LVP formation and increase IM production; however, unlike *hand2* loss of function, elevated *osr1* expression does not also convert the *hand2*-expressing lateral posterior mesoderm into Pax2a$^+$ IM.

Because *osr1* overexpression at tailbud was sufficient to increase IM formation, we wondered when *osr1* function is normally required to promote IM and pronephron development. Other studies have implicated *osr1* in mesendoderm development prior to gastrulation: notably, *osr1* knockdown resulted in increased formation of endoderm progenitors in the early embryo, suggesting a possible influence of excess endoderm on IM development (Mudumana et al., 2008; Terashima et al., 2014). We found milder endoderm phenotypes in *osr1* mutants (Fig. S9): we observed a trend toward a mild increase in endoderm progenitors at shield stage (Fig. S9A,B); however, unlike previous observations in *osr1* morphants (Mudumana et al., 2008), we did not observe an increased amount of endoderm at the 18-somite stage (Fig. S9C,D). Because previous work suggested that *osr1* acts during the earliest stages of endoderm differentiation to inhibit the formation of endoderm progenitors (Terashima et al., 2014), we chose to assess when induction of *osr1* expression is able to rescue the *osr1* mutant defects. Induction of *osr1* expression at tailbud clearly rescued the *osr1* mutant IM, podocyte and pronephron tubule defects (Fig. 4H-P). Thus, *osr1* function after gastrulation is sufficient to regulate IM development, and *osr1* function during earlier stages of mesendoderm development is not absolutely required for proper IM and pronephron formation. Conversely, induction of *osr1* at the 10-somite stage failed to rescue the pronephron defects in *osr1* mutants (Fig. 4P). Together, our analyses suggest a timeframe after the completion of gastrulation during which *osr1* function is sufficient to promote the development of pronephron progenitors within the IM. Intriguingly, the timepoint at which *osr1* induction was no longer able to rescue pronephron development coincides with the normal timing of LVP emergence.

osr1 acts in opposition to hand2 to promote IM differentiation while inhibiting LVP emergence

Altogether, our studies provide new insights into the roles of *osr1* in IM and vessel progenitor development. We show that *osr1* is both necessary and sufficient to promote the initial differentiation of some, but not all, IM. In addition, we reveal context-dependent roles for *osr1* in inhibiting vessel progenitor development, including an intriguing role in preventing the premature appearance of vessel progenitors at the lateral border of the IM. Finally, our findings suggest that the dynamic nature of *osr1* expression in the posterior mesoderm is necessary for balancing the extent of IM formation with the timing of neighboring LVP emergence.

How might *osr1* regulate both the IM and LVP lineages within the posterior mesoderm? Our findings indicate the presence of a unique territory at the boundary between the developing IM and the laterally adjacent mesoderm in which *osr1* initially acts in opposition to *hand2* to promote IM differentiation while inhibiting vessel progenitor differentiation; later, as *osr1* expression recedes, IM differentiation ceases and vessel progenitors emerge. Conceptually, we envision that the dynamic levels of *osr1* expression couple developmental timing with cell fate acquisition in order to set boundaries that delineate the extent of each progenitor territory. In future studies, it will be important to determine how directly or indirectly Osr1 and Hand2 regulate expression of the downstream genes that control IM and vessel identity, such as *pax2a* and *etv2*. Previous work suggested that Osr1 and its *Drosophila* homolog Odd function as transcriptional repressors (Goldstein et al., 2005; Tena et al., 2007). Considering the importance of reciprocal repressor interactions in establishing boundaries between neighboring progenitor territories in other developmental contexts (Briscoe and Small, 2015), it is interesting to speculate that, in the posterior mesoderm, a key function of Osr1 is to repress LVP formation while a primary role of Hand2 is to inhibit IM differentiation.

Our studies also suggest three subregions capable of contributing to the IM, arranged along the medial-lateral axis of zebrafish posterior mesoderm, with distinct genetic networks regulating IM formation in each area: a medial *osr1*-independent territory; a far lateral territory with latent IM-forming potential that is repressed by the sustained expression of *hand2*; and a boundary territory in between these in which a balance between *hand2* and *osr1* determines the precise amount and timing of IM and LVP formation. High-resolution lineage tracing will be necessary to delineate the precise fate map within the posterior mesoderm. Furthermore, it remains unknown whether *hand2* and *osr1* act cell-autonomously within the boundary territory to direct the fate of progenitors with the potential to contribute to the IM or LVP lineages. Considering the ectopic appearance of Pax2a within *hand2*-expressing cells in *hand2* mutants (Fig. S8C; Perens et al., 2016), we hypothesize that *hand2* acts cell-autonomously to regulate a decision between IM and LVP fates. Likewise, it is appealing to propose that *osr1* acts in the same manner as *hand2*. In addition to being expressed in the same territory (Fig. 3J-O; Perens et al., 2016), *osr1* and *hand2* seem to function in the same
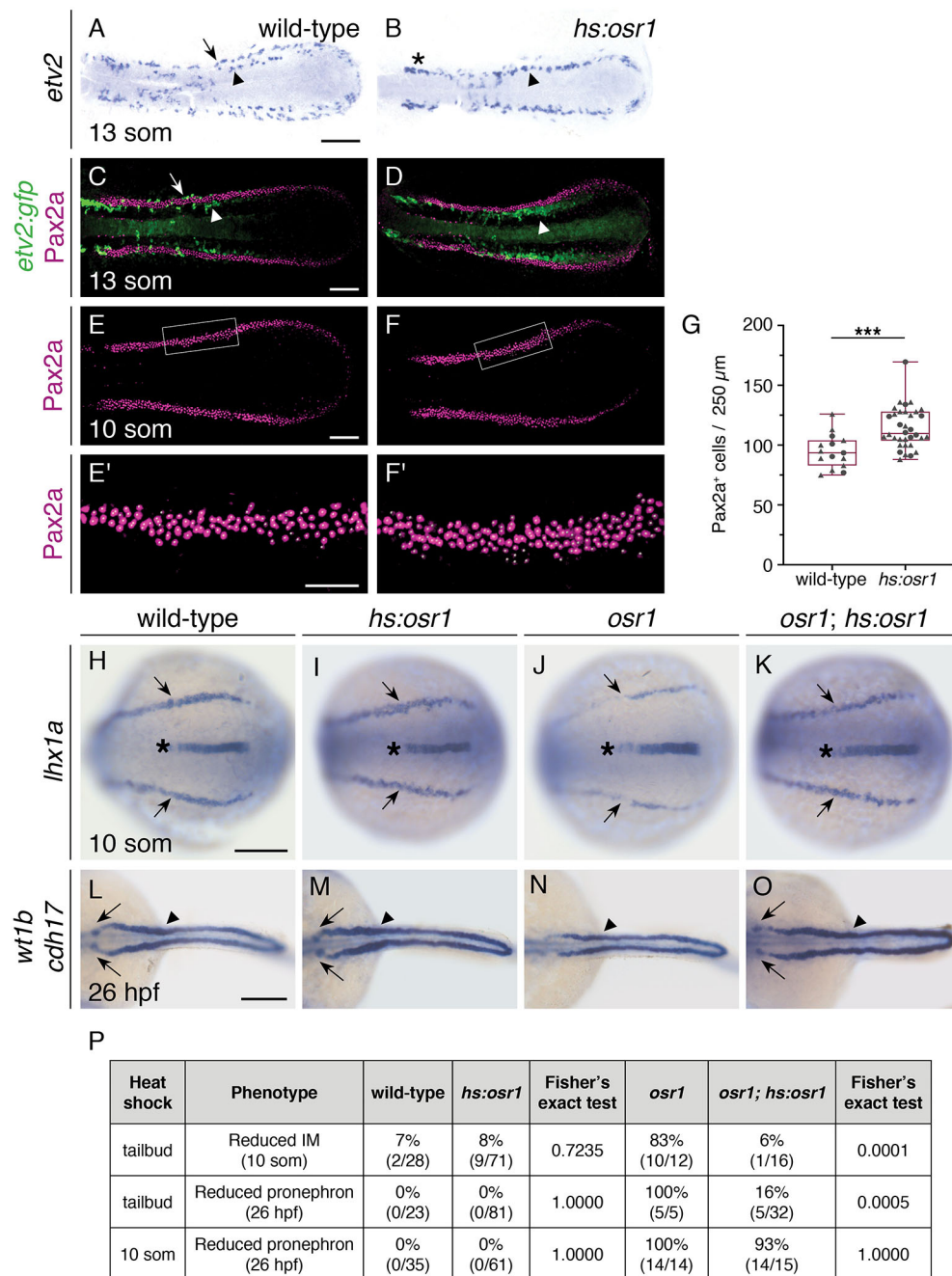
Fig. 4. Increased *osr1* expression inhibits lateral vessel progenitor emergence and elevates IM formation. *In situ* hybridization (A,B,H-O) and immunofluorescence (C-F) indicate expression patterns in the posterior mesoderm; dorsal views, anterior to the left. (A,B) In contrast to wild-type embryos (A), which display *etv2* expression in both medial (arrowhead) and lateral (arrow) territories, *Tg(hsp70:osr1-t2A-BFP)* (*hs:osr1*) embryos (B) display increased expression of *etv2* in medial (arrowhead) and proximal (asterisk) territories, but decreased *etv2* expression in lateral territories at the 13-somite stage (som). (C-F) Three-dimensional reconstructions of Pax2a and GFP immunofluorescence in wild-type (C,E) and *hs:osr1* (D,F) embryos carrying *Tg(etv2:egfp)*. While *etv2:egfp* expression is seen in both medial (arrowhead) and lateral (arrow) territories in wild-type at 13 som (C), *etv2:egfp* expression is seen only in a wide territory medial to the Pax2a⁺ IM in *hs:osr1* embryos (D, arrowhead). (E-G) Quantification of Pax2a⁺ cells, as in Fig. 2E-I, demonstrates a significant increase in IM cells in *hs:osr1* embryos. Symbols represent individual embryos (circles, average of left and right IMs; triangles, single IM; see Materials and Methods); boxes represent interquartile range; central line marks the median; whiskers indicate maximum and minimum values. *P* values were calculated using non-parametric Mann–Whitney *U*-tests: ***P=0.002. (H-O) Induction of *osr1* expression at tailbud rescues IM and pronephron defects in *osr1* mutants. Wild-type and *osr1* mutant embryos carrying *hs:osr1* were compared with their nontransgenic siblings; heat shock was performed at tailbud in all embryos shown. Unlike the reduced expression in *osr1* mutants (J), *lhx1a* expression in the IM of *osr1;hs:osr1* embryos (K) is comparable with wild type (H) and *hs:osr1* (I) at 10 som; expression in the notochord (asterisks) was unaffected. Unlike the absent *wt1b* expression in the glomerular precursors (arrows) and the decreased *cdh17* expression in the pronephron tubule (arrowheads) in *osr1* mutants (N), *wt1b* and *cdh17* expression in *osr1;hs:osr1* (O) are comparable with wild type (L) and *hs:osr1* (M). (P) Numbers of embryos exhibiting *osr1* mutant phenotypes, as shown in J,N. Proportions of individuals with a mutant appearance were compared between embryos carrying *hs:osr1* and their corresponding nontransgenic siblings using Fisher's exact test; *P* values are provided for each comparison. Notably, induction of *osr1* expression at tailbud, but not at 10 som, rescued *osr1* mutant phenotypes. Scale bars: 100 μm (A-E,F,H-O); 50 μm (E′,F′).

timeframe: the stage after which induction of *osr1* expression fails to rescue the *osr1* mutant pronephron defects (Fig. 4P) coincides with the stage after which *hand2* overexpression fails to inhibit pronephron development (Perens et al., 2016). Alternatively, instead of functioning autonomously within progenitor cells in the boundary territory, either *hand2* or *osr1* may influence IM and LVP cell fate decisions by controlling the production of diffusible signals that pattern the medial-lateral axis of the posterior mesoderm. Others have suggested that *osr1* regulates the development of pronephron and vessel lineages non-autonomously, through its function during early endoderm development (Mudumana et al., 2008; Tomar et al., 2014). Our demonstration that induction of *osr1* expression at tailbud can rescue the *osr1* mutant phenotype argues against a mechanism in which *osr1* regulates pronephron development by controlling the initial formation of endoderm progenitors; however, we cannot rule out a later role for *osr1* in the endoderm. Ultimately, mosaic analysis will be necessary to determine where Osr1 and Hand2 function to shape the developmental potential of specific territories within the posterior mesoderm.

In the long term, an understanding of the impact of *osr1* on medial-lateral patterning of the posterior mesoderm may have important implications for understanding congenital anomalies of the kidney and urinary tract (CAKUT), as *OSR1* mutations have been associated with CAKUT phenotypes, including renal hypoplasia and vesicoureteral reflux (Fillion et al., 2017; Zhang et al., 2011). Additionally, because generation of IM is a key step in the production of vascularized kidney organoids (Takasato et al., 2015), *in vivo* analyses of *osr1* function during IM and vessel progenitor formation have the potential to inform future refinements of relevant *in vitro* differentiation protocols.

MATERIALS AND METHODS
Zebrafish
We generated embryos by breeding wild-type zebrafish, zebrafish heterozygous for the *osr1* mutant allele *osr1*[el593] (RRID: ZFIN_ZDB-ALT-171010-14) (Askary et al., 2017), zebrafish heterozygous for the *hand2* mutant allele *han*[s6] (RRID: ZFIN_ZDB-GENO-071003-2) (Yelon et al., 2000), and zebrafish carrying *Tg(hand2:egfp)*[pd24] (RRID: ZFIN_ZDB-GENO-110128-35) (Kikuchi et al., 2011), *Tg(hsp70:osr1-t2A-BFP)*[sd63] or *Tg(etv2:egfp)*[ci1] (RRID: ZFIN_ZDB-GENO-110131-58) (Proulx et al., 2010). For induction of heat shock-regulated expression, embryos were placed at 37°C for 1 h and then returned to 28°C. All heat shocks were performed at tailbud, except for those described in Fig. 4P, which were performed at the 10-somite stage. Following heat shock, transgenic embryos were identified based on BFP fluorescence; embryos used for cell counting in Fig. 4E-G were confirmed to carry the transgene by PCR genotyping for the *bfp*-coding region, using the primers 5′-CTGGAAGGCAGAAACGACAT-3′ and 5′-TGCTAGGGAGGTCGCA-GTAT-3′. Nontransgenic embryos were analyzed as controls. PCR genotyping was conducted as previously described for *osr1*[el593] mutants (Askary et al., 2017), for *han*[s6] mutants (Yelon et al., 2000) and for *han*[s6] mutants containing *Tg(hand2:EGFP)*[pd24] (Perens et al., 2016). For *osr1*[el593] mutants containing *Tg(hsp70:osr1-t2A-BFP)*, we used a primer pair that would only amplify the endogenous *osr1* locus, followed by digestion with EarI: 5′-AATGTTCTCTCTGTTTGTGTCTCC-3′ and 5′-AGGTTGG-CAAAGTCAAAACG-3′. All zebrafish work followed protocols approved by the UCSD IACUC.

Creation of stable transgenic lines
To generate transgenes for heat-activated overexpression of *osr1*, we first amplified the *osr1*-coding sequence from pCS2-*osr1* (Mudumana et al., 2008), using the primers 5′-AAAAAAGCAGGCTGCCACCGATGGG-TAGTAAGACGCTC-3′ and 5′-CTCCTCCGGACCCGCCGCCGTACTT-TATCTTGGCTGGC-3′, and cloned the amplicon into the vector *hsp70*-BamHI-t2a-BFP at the BamHI restriction site. We employed standard

protocols to create transgenic founders (Fisher et al., 2006). The F1 progeny of prospective founder fish were screened for BFP fluorescence following heat shock for 1 h at 37°C, and phenotypic analysis was performed on the F1 and F2 progeny of three separate founders carrying distinct integrations of *Tg(hsp70:osr1-t2A-BFP)*. Similar phenotypes were observed in all three transgenic lines; data shown in Figs 4, S5, S7 and S8 depict results from the line *Tg(hsp70:osr1-t2A-BFP)*[sd63].

Injection
We synthesized capped mRNA from a pCS2-*osr1* plasmid using the Ambion mMESSAGE mMACHINE kit, and injected 64 ng into embryos at the one-cell stage. To knock down *sox32* function, we injected 3.4 ng of a previously characterized translation-blocking *sox32* morpholino at the one-cell stage (Dickmeis et al., 2001).

In situ hybridization
Standard whole-mount *in situ* hybridization were performed as previously described (Thomas et al., 2008) using the following probes: *atp1a1a.4* (ZDB-GENE-001212-4), *cdh17* (ZDB-GENE-030910-3), *etv2* (*etsrp*; ZDB-GENE- 050622-14), *flk1* (*kdrl*; ZDB-GENE-000705-1), *flt4* (ZDB-GENE-980526-326), *foxa2* (ZDB-GENE-980526-404), *gata1* (ZDB-GENE-980536-268), *hand2* (ZDB-GENE- 000511-1), *lhx1a* (*lim1*; ZDB-GENE-980526-347), *mrc1a* (ZDB-GENE-090915-4), *osr1* (ZDB-GENE-070321-1), *pax2a* (ZDB-GENE-990415-8), *slc12a3* (ZDB-GENE-030131-9505), *slc20a1a* (ZDB-GENE-040426-2217), *sox17* (ZDB-GENE-991213-1) and *wt1b* (ZDB-GENE-050420-319).

Immunofluorescence
Whole-mount immunofluorescence was performed as previously described (Cooke et al., 2005), using polyclonal antibodies against Pax2a at 1:100 dilution (Genetex, GTX128127) (RRID: AB_2630322) and against GFP at 1:250 dilution (Life Technologies, A10262) (RRID: AB_2534023), together with the secondary antibodies goat anti-chick Alexa Fluor 488 (Life Technologies, A11039) (RRID: AB_2534096) and goat anti-rabbit Alexa Fluor 594 (Life Technologies, A11012) (RRID: AB_10562717), both at 1:100 dilution. Samples were then placed in SlowFade Gold anti-fade reagent (Life Technologies) and mounted in 50% glycerol.

Imaging
Bright-field images were captured with a Zeiss Axiocam on a Zeiss Axiozoom microscope and processed using Zeiss AxioVision. Confocal images were collected by a Leica SP5 or SP8 confocal laser-scanning microscope using a 10× dry objective and a slice thickness of 1 μm, and analyzed using Imaris software (Bitplane).

Cell counting
To count Pax2a^{+} cells, we flat-mounted and imaged embryos after dissecting away the yolk and the anterior region of the embryo. We examined a representative 250 μm long region in roughly the middle of the IM, selecting contiguous regions that were unaffected by dissection artifacts. When the quality of the dissection allowed both the right and left sides of the embryo to be counted, we counted Pax2a^{+} cells on both sides and represented the embryo by the average of the two values; otherwise, only one side was counted. In all cases, Pax2a^{+} cells were identified through examination of both three-dimensional reconstructions and individual optical sections. To differentiate Pax2a^{+} cells from background immunofluorescence, we used Imaris to decrease brightness until staining clearly outside of IM was no longer visible.

Statistics and replication
Statistical analysis was performed using Graphpad Prism 8 to conduct non-parametric Mann–Whitney *U*-tests when data involved a continuous variable. Fisher's exact test was used when data involved categorical variables. All results represent at least two independent experiments (technical replicates) in which multiple embryos, from multiple independent matings, were analyzed (biological replicates). For wild-type and mutant *in situ* hybridization results for which the phenotype was not quantified,

phenotypes shown are representative examples from at least 10 embryos for wild-type and *osr1* mutant phenotypes, and from at least five embryos for *hand2* mutant and *hand2*; *osr1* double mutant phenotypes. For wild-type, transgenic and mutant antibody staining results for which the phenotype was not quantified (Fig. 4C,D, Fig. S8), phenotypes shown are representative examples from at least five embryos.

References

Askary, A., Xu, P., Barske, L., Bay, M., Bump, P., Balczerski, B., Bonaguidi, M. A. and Crump, J. G. (2017). Genome-wide analysis of facial skeletal regionalization in zebrafish. *Development* **144**, 2994-3005.

Briscoe, J. and Small, S. (2015). Morphogen rules: design principles of gradient-mediated embryo patterning. *Development* **142**, 3996-4009. doi:10.1242/dev.129452

Carroll, T. J., Wallingford, J. B. and Vize, P. D. (1999). Dynamic patterns of gene expression in the developing pronephros of Xenopus laevis. *Dev. Genet.* **24**, 199-207. doi:10.1002/(SICI)1520-6408(1999)24:3/4<199::AID-DVG3>3.0.CO;2-D

Cirio, M. C., Hui, Z., Haldin, C. E., Cosentino, C. C., Stuckenholz, C., Chen, X., Hong, S. K., Dawid, I. B. and Hukriede, N. A. (2011). Lhx1 is required for specification of the renal progenitor cell field. *PLoS ONE* **6**, e18858. doi:10.1371/journal.pone.0018858

Cooke, J. E., Kemp, H. A. and Moens, C. B. (2005). EphA4 is required for cell adhesion and rhombomere-boundary formation in the zebrafish. *Curr. Biol.* **15**, 536-542. doi:10.1016/j.cub.2005.02.019

Davidson, A. J., Lewis, P., Przepiorski, A. and Sander, V. (2019). Turning mesoderm into kidney. *Semin. Cell Dev. Biol.* **91**, 86-93. doi:10.1016/j.semcdb.2018.08.016

Dickmeis, T., Mourrain, P., Saint-Etienne, L., Fischer, N., Aanstad, P., Clark, M., Strahle, U. and Rosa, F. (2001). A crucial component of the endoderm formation pathway, CASANOVA, is encoded by a novel sox-related gene. *Genes Dev.* **15**, 1487-1492. doi:10.1101/gad.196901

Dressler, G. R. (2009). Advances in early kidney specification, development and patterning. *Development* **136**, 3863-3874. doi:10.1242/dev.034876

Drummond, B. E., Chambers, B. E., Wesselman, H. M., Ulrich, M. N., Gerlach, G. F., Kroeger, P. T., Jr., Leshchiner, I., Goessling, W. and Wingert, R. A., (2020). osr1 maintains renal progenitors and regulates podocyte development by promoting wnt2ba through antagonism of hand2. *bioRxiv* doi:10.1101/2020.12.21.423845

Fillion, M. L., El Andalousi, J., Tokhmafshan, F., Murugapoopathy, V., Watt, C. L., Murawski, I. J., Capolicchio, J. P., El-Sherbiny, M., Jednak, R. and Gupta, I. R. (2017). Heterozygous loss-of-function mutation in Odd-skipped related 1 (Osr1) is associated with vesicoureteric reflux, duplex systems, and hydronephrosis. *Am. J. Physiol. Renal. Physiol.* **313**, F1106-F1115. doi:10.1152/ajprenal.00107.2017

Fisher, S., Grice, E. A., Vinton, R. M., Bessling, S. L., Urasaki, A., Kawakami, K. and McCallion, A. S. (2006). Evaluating the biological relevance of putative enhancers using Tol2 transposon-mediated transgenesis in zebrafish. *Nat. Protoc.* **1**, 1297-1305. doi:10.1038/nprot.2006.230

Gerlach, G. F. and Wingert, R. A. (2013). Kidney organogenesis in the zebrafish: insights into vertebrate nephrogenesis and regeneration. *Wiley Interdiscip Rev. Dev. Biol.* **2**, 559-585. doi:10.1002/wdev.92

Goldstein, R. E., Cook, O., Dinur, T., Pisante, A., Karandikar, U. C., Bidwai, A. and Paroush, Z. (2005). An eh1-like motif in odd-skipped mediates recruitment of Groucho and repression in vivo. *Mol. Cell. Biol.* **25**, 10711-10720. doi:10.1128/MCB.25.24.10711-10720.2005

James, R. G., Kamei, C. N., Wang, Q., Jiang, R. and Schultheiss, T. M. (2006). Odd-skipped related 1 is required for development of the metanephric kidney and regulates formation and differentiation of kidney precursor cells. *Development* **133**, 2995-3004. doi:10.1242/dev.02442

Kikuchi, K., Holdway, J. E., Major, R. J., Blum, N., Dahn, R. D., Begemann, G. and Poss, K. D. (2011). Retinoic acid production by endocardium and epicardium is an injury response essential for zebrafish heart regeneration. *Dev. Cell* **20**, 397-404. doi:10.1016/j.devcel.2011.01.010

Kohli, V., Schumacher, J. A., Desai, S. P., Rehn, K. and Sumanas, S. (2013). Arterial and venous progenitors of the major axial vessels originate at distinct locations. *Dev. Cell* **25**, 196-206. doi:10.1016/j.devcel.2013.03.017

Kroeger, P. T., Jr, Drummond, B. E., Miceli, R., McKernan, M., Gerlach, G. F., Marra, A. N., Fox, A., McCampbell, K. K., Leshchiner, I., Rodriguez-Mari, A. et al. (2017). The zebrafish kidney mutant zeppelin reveals that brca2/fancd1 is essential for pronephros development. *Dev. Biol.* **428**, 148-163. doi:10.1016/j.ydbio.2017.05.025

Lun, K. and Brand, M. (1998). A series of no isthmus (noi) alleles of the zebrafish pax2.1 gene reveals multiple signaling events in development of the midbrain-hindbrain boundary. *Development* **125**, 3049-3062. doi:10.1242/dev.125.16.3049

Mudumana, S. P., Hentschel, D., Liu, Y., Vasilyev, A. and Drummond, I. A. (2008). . odd skipped related1 reveals a novel role for endoderm in regulating kidney versus vascular cell fate. *Development* **135**, 3355-3367. doi:10.1242/dev.022830

Mugford, J. W., Sipila, P., McMahon, J. A. and McMahon, A. P. (2008). Osr1 expression demarcates a multi-potent population of intermediate mesoderm that undergoes progressive restriction to an Osr1-dependent nephron progenitor compartment within the mammalian kidney. *Dev. Biol.* **324**, 88-98. doi:10.1016/j.ydbio.2008.09.010

Perens, E. A., Garavito-Aguilar, Z. V., Guio-Vega, G. P., Pena, K. T., Schindler, Y. L. and Yelon, D. (2016). Hand2 inhibits kidney specification while promoting vein formation within the posterior mesoderm. *Elife* **5**, e19941. doi:10.7554/eLife.19941

Proulx, K., Lu, A. and Sumanas, S. (2010). Cranial vasculature in zebrafish forms by angioblast cluster-derived angiogenesis. *Dev. Biol.* **348**, 34-46. doi:10.1016/j.ydbio.2010.08.036

Prummel, K. D., Nieuwenhuize, S. and Mosimann, C. (2020). The lateral plate mesoderm. *Development* **147**, dev175059. doi:10.1242/dev.175059

Schulte-Merker, S. and Stainier, D. Y. (2014). Out with the old, in with the new: reassessing morpholino knockdowns in light of genome editing technology. *Development* **141**, 3103-3104. doi:10.1242/dev.112003

Takasato, M., Er, P. X., Chiu, H. S., Maier, B., Baillie, G. J., Ferguson, C., Parton, R. G., Wolvetang, E. J., Roost, M. S., Chuva de Sousa Lopes, S. M. et al. (2015). Kidney organoids from human iPS cells contain multiple lineages and model human nephrogenesis. *Nature* **526**, 564-568. doi:10.1038/nature15695

Tena, J. J., Neto, A., de la Calle-Mustienes, E., Bras-Pereira, C., Casares, F. and Gomez-Skarmeta, J. L. (2007). Odd-skipped genes encode repressors that control kidney development. *Dev. Biol.* **301**, 518-531. doi:10.1016/j.ydbio.2006.08.063

Terashima, A. V., Mudumana, S. P. and Drummond, I. A. (2014). Odd skipped related 1 is a negative feedback regulator of nodal-induced endoderm development. *Dev. Dyn.* **243**, 1571-1580. doi:10.1002/dvdy.24191

Thomas, N. A., Koudijs, M., van Eeden, F. J., Joyner, A. L. and Yelon, D. (2008). Hedgehog signaling plays a cell-autonomous role in maximizing cardiac developmental potential. *Development* **135**, 3789-3799. doi:10.1242/dev.024083

Tomar, R., Mudumana, S. P., Pathak, N., Hukriede, N. A. and Drummond, I. A. (2014). osr1 Is Required for Podocyte Development Downstream of wt1a. *J. Am. Soc. Nephrol.* **25**, 2539-2545. doi:10.1681/ASN.2013121327

Torres, M., Gomez-Pardo, E., Dressler, G. R. and Gruss, P. (1995). Pax-2 controls multiple steps of urogenital development. *Development* **121**, 4057-4065. doi:10.1242/dev.121.12.4057

Tsang, T. E., Shawlot, W., Kinder, S. J., Kobayashi, A., Kwan, K. M., Schughart, K., Kania, A., Jessell, T. M., Behringer, R. R. and Tam, P. P. (2000). Lim1 activity is required for intermediate mesoderm differentiation in the mouse embryo. *Dev. Biol.* **223**, 77-90. doi:10.1006/dbio.2000.9733

Wang, Q., Lan, Y., Cho, E. S., Maltby, K. M. and Jiang, R. (2005). Odd-skipped related 1 (Odd 1) is an essential regulator of heart and urogenital development. *Dev. Biol.* **288**, 582-594. doi:10.1016/j.ydbio.2005.09.024

Yelon, D., Ticho, B., Halpern, M. E., Ruvinsky, I., Ho, R. K., Silver, L. M. and Stainier, D. Y. (2000). The bHLH transcription factor hand2 plays parallel roles in zebrafish heart and pectoral fin development. *Development* **127**, 2573-2582. doi:10.1242/dev.127.12.2573

Zhang, Z., Iglesias, D., Eliopoulos, N., El Kares, R., Chu, L., Romagnani, P. and Goodyer, P. (2011). A variant OSR1 allele which disturbs OSR1 mRNA expression in renal progenitor cells is associated with reduction of newborn kidney size and function. *Hum. Mol. Genet.* **20**, 4167-4174. doi:10.1093/hmg/ddr341

DEVELOPMENT